

## Pathways of Electron Transfer in *Escherichia coli* DNA Photolyase: Trp<sup>306</sup> to FADH

Margaret S. Cheung,\* Iraj Daizadeh,\* A. A. Stuchebrukhov,\* and Paul F. Heelis#

\*Department of Chemistry, University of California, Davis, California 95616, USA, and #North East Wales Institute, Mold Road, Wrexham, Clwyd LL11 2AW, Wales

**ABSTRACT** We describe the results of a series of theoretical calculations of electron transfer pathways between Trp<sup>306</sup> and \*FADH' in the *Escherichia coli* DNA photolyase molecule, using the method of interatomic tunneling currents. It is found that there are two conformationally orthogonal tryptophans, Trp<sup>359</sup> and Trp<sup>382</sup>, between donor and acceptor that play a crucial role in the pathways of the electron transfer process. The pathways depend vitally on the aromaticity of tryptophans and the flavin molecule. The results of this calculation suggest that the major pathway of the electron transfer is due to a set of overlapping orthogonal  $\pi$ -rings, which starts from the donor Trp<sup>306</sup>, runs through Trp<sup>359</sup> and Trp<sup>382</sup>, and finally reaches the flavin group of the acceptor complex, FADH.

### INTRODUCTION

Far-UV light (200–300 nm) is harmful to the biological function of DNA. Its action results in the formation of cyclobutane thymine dimers, which are the major photo-products in the damaged DNA by UV irradiation (Harm, 1980; Sancar, 1994; Kim and Sancar, 1993; Heelis et al., 1995). A cyclobutane thymine dimer is created by the linkage of two neighboring thymine bases via C5–C5 and C6–C6 atoms. The loss of aromaticity of these dimerized thymines weakens the hydrogen bonding between base pairs. In addition, the cyclobutane bond perturbs the structure of DNA, thus creating a “kink” in the helical axis (Husain et al., 1988; Miaskiewicz et al., 1996). This lesion will further block replication and transcription, which leads to cytotoxic and mutagenic effects (Harm, 1980).

To maintain genetic stability, cells protect themselves against these types of damage by several repair mechanisms. One of these mechanisms is photoreactivation (Kim and Sancar, 1993; Sancar, 1994, 1996). A photoreactivating enzyme, DNA photolyase, selectively binds to a damaged part of DNA, absorbs lower-energy photons of near-UV and visible light (300–500 nm), and reverses the dimer into individual thymines (Sancar, 1994). Photolyases and their homologs are widespread in nature; the mechanism of their action and their biological function are subjects of intense research (Kanai et al., 1997; Todo et al., 1996; Özer et al., 1995).

Recently, the crystal structure of DNA photolyase from *Escherichia coli* has been resolved (Park et al., 1995). *E. coli* photolyase is a monomeric protein of 471 amino acids. It includes two noncovalently attached cofactors. *E. coli* is regarded as a folate class enzyme that contains the blue

light harvest cofactor, 5,10-methenyltetrahydrofolylpolyglutamate (MTHF) (Johnson et al., 1988). The other catalytic cofactor is 7,8-didemethyl-8-hydroxy-5-deazariboflavin (FADH<sup>-</sup>) (Payne et al., 1987). From the crystal structure of photolyase, a U-shaped FADH<sup>-</sup> is located in a “hole” that may act like the active site accessible for docking with the dimer.

Current data support the following major steps in the photorepair mechanism. Photolyase selectively binds to the dimer in a light-independent step (Sancar et al., 1985; Kim and Sancar, 1991), and the MTHF cofactor absorbs a blue light photon and then excites FADH<sup>-</sup>, by energy transfer (Kim et al., 1993; Payne et al., 1987). The excited FADH<sup>-</sup>, \*FADH<sup>-</sup>, transfers an electron to split the dimer (Kim et al., 1993; Payne et al., 1987; Kim and Sancar, 1993), the electron is transferred back to photolyase, and the intact DNA dissociates. There are variations in the mechanism for splitting the dimer. From experiment, for example, it is known that Trp<sup>277</sup> can absorb a 280-nm photon and thereby split the dimer by a direct electron transfer (ET) reaction (Kim et al., 1992).

Under purification conditions, the flavin molecule oxidizes into the neutral form and becomes catalytically inert. Under the irradiation with white light, however, the photolyase regains its ability to reduce the dimer (Kim and Sancar, 1993). It has been suggested that the return of the activity of photolyase is due to a Trp<sup>306</sup>-to-\*FADH' electron transfer. The evidence for this mechanism comes from time-resolved electron paramagnetic resonance experiments (Kim et al., 1993) and site-specific mutagenesis studies (Li et al., 1991).

Experimentally it has been shown that the neutral radical form of FADH can be excited by absorption of a photon to produce \*FADH' (~510 nm), and \*FADH' can be reduced to the catalytic active form \*FADH<sup>-</sup> by Trp<sup>306</sup>, which is located close to the surface of the enzyme and ~14 Å away from the flavin. Trp<sup>306</sup> is not the closest tryptophan to FADH and, given the large distance from the flavin, is not directly coupled to FADH. This suggests that there are intermediates (virtual or real) between Trp<sup>306</sup> and FADH

Received for publication 15 May 1998 and in final form 9 November 1998.

Address reprint requests to Dr. A. A. Stuchebrukhov, Department of Chemistry, University of California, One Shields Avenue, Davis, CA 95616. Tel.: 530-752-7778; Fax: 530-752-8995; E-mail: stuchebr@chem.ucdavis.edu.

© 1999 by the Biophysical Society

0006-3495/99/03/1241/09 \$2.00

that would be interesting to identify. Several pathways for this electron transfer can be proposed on the basis of the crystal structure (Park et al., 1995). However, the qualitative visual analysis is ambiguous, because there are gaps in the tertiary structure and there are no direct secondary structures that connect Trp<sup>306</sup> to FADH. Moreover, unlike other cases of electron transfer in proteins, such as azurin or cytochrome *c* (Casimiro et al., 1993; Langen et al., 1995; Onuchic et al., 1992), photolyase lacks metal atoms serving as well-defined donor and acceptor sites. This also adds to the uncertainty of assigning the tunneling path in the qualitative analysis.

In this paper, we describe results of theoretical calculations of ET pathways between Trp<sup>306</sup> and FADH with the recently developed method of atomic tunneling currents (Stuchebrukhov, 1996). We find that two conformationally orthogonal tryptophans, Trp<sup>359</sup> and Trp<sup>382</sup>, between donor and acceptor play a crucial role in the pathways of electron transfer. The pathways depend vitally on the aromaticity of tryptophans and the flavin molecule. The results of this calculation suggest that the major pathway of the electron transfer is through a set of orthogonal  $\pi$ -rings that starts from the donor Trp<sup>306</sup>, runs through Trp<sup>359</sup> and Trp<sup>382</sup>, and finally reaches the acceptor complex, FADH, through one of the methyl groups of the flavin molecule.

This paper is structured as follows. The first section is an overview of Marcus's theory of electron transfer (Marcus and Sutin, 1985) and computational methods for evaluating the rate constant by a semiempirical extended Hückel method. In the second section we introduce the pruning technique, the purpose of which is to identify the most important amino acids in the protein (Gehlen et al., 1996). These amino acids constitute the tunneling pathway at the amino acid level of resolution. In the third section we describe the method of atomic tunneling currents, which yields the atomic details of electron transfer pathways between Trp<sup>306</sup> and FADH. In the last section, we discuss results and propose further steps of theoretical analysis of the function of photolyase.

## THEORETICAL BACKGROUND

### Rate of ET reaction

The rate of an electron transfer (ET) reaction is given by a product of electronic and nuclear factors (Marcus and Sutin, 1985; Kuznetsov, 1995):

$$k_{\text{ET}} = \frac{2\pi}{\hbar} |T_{\text{DA}}|^2 \rho_{\text{FC}} \quad (1)$$

In this expression,  $T_{\text{DA}}$  is the electronic coupling of donor and acceptor complexes, and  $\rho_{\text{FC}}$  is the Franck-Condon density of states. According to Marcus's theory, electron transfer occurs when a favorable thermal fluctuation of the polar solvent environment or that of the nuclear coordinates of the donor and acceptor complexes shifts the donor and acceptor electronic states into resonance. Such a resonance

is the transition state for the ET reaction. The factor  $\rho_{\text{FC}}$  in the above formula is proportional to the frequency of the occurrence of the transition state in the system, and the electronic factor  $|T_{\text{DA}}|^2$  determines the probability that once at the transition state an electron transfer will occur.

The nuclear factor  $\rho_{\text{FC}}$  depends on the reorganization energy  $\lambda$ , the driving force of the reaction  $\Delta G^0$ , and the temperature  $T$  and, in the classical approximation, is given by the well-known Marcus expression:

$$\rho_{\text{FC}} = \frac{1}{\sqrt{4\pi\lambda k_{\text{B}}T}} \exp\left(-\frac{(\Delta G^0 + \lambda)^2}{4\lambda k_{\text{B}}T}\right) \quad (2)$$

The electronic coupling is determined by the structure of the protein medium intervening between donor and acceptor complexes and by their distance. When donor and acceptor are not in direct van der Waals contact, certain structural units of the protein, which are usually close to a straight line connecting donor and acceptor, play the role of the bridge for electron transfer. When the bridging elements are not real intermediates, the electronic coupling is due to superexchange (McConnell, 1961). In such a case the long-distance electron transfer between donor and acceptor occurs via quantum mechanical tunneling, and the bridging elements provide important virtual intermediates in superexchange coupling. Superexchange has been identified as the major mechanism for long-distance electron coupling in proteins (Onuchic et al., 1992; Casimiro et al., 1993; Langen et al., 1995). The sequence of virtual intermediate transitions constitutes the tunneling pathway.

The superexchange coupling matrix element  $T_{\text{DA}}$  can be evaluated by using the perturbation theory expression (see, for example, Stuchebrukhov, 1997):

$$T_{\text{DA}} = \sum_{ij} V_{\text{ai}} G_{ij} V_{\text{jd}}, \quad (3)$$

where  $V_{\text{ai}}$  and  $V_{\text{jd}}$  are the couplings of the donor and acceptor electronic states to the bridge states,  $i, j$ , and  $G_{ij}$  is the electronic Green's function of the bridge. The above expression only gives an approximate value of the coupling matrix element—in the derivation it is assumed that the coupling to the bridge is small. Typically, however, a more exact treatment gives a correction factor on the order of unity (Katz and Stuchebrukhov, 1998). The above expression can be evaluated if the Hamiltonian of the system is known.

### Extended Hückel Hamiltonian

In the present calculation the semiempirical extended Hückel method is employed. For a given set of atomic coordinates of the protein (taken from the crystallographic data), the Hamiltonian matrix is constructed in the following way. Each atom is assigned a number of Slater-type atomic orbitals. Only valence states are considered. Hydrogen has one  $s$  orbital, and the other atoms have four (one  $s$

and three  $p$ ) orbitals. Because there are no metal atoms in photolyase, no  $d$  orbitals are involved in the calculation.

The ionization potentials of these valence states are the diagonal matrix elements of the Hamiltonian,  $H_{ii} = I_i$ . These values, as well as parameters of radial Slater-type functions for the orbitals, were taken from a standard extended Hückel program (Whangbo et al., 1976). The atomic basis set is not orthogonal, and the corresponding overlap matrix  $S_{ij}$  is calculated for a given set of atomic coordinates of the protein. The nondiagonal matrix elements of the Hamiltonian matrix are calculated using Wolfsberg-Helmholz parameterization:

$$H_{ij} = KS_{ij} \left( \frac{H_{ii} + H_{jj}}{2} \right), \quad (4)$$

where  $S_{ij}$  is the corresponding element of the overlap matrix, the empirical parameter  $K$  is chosen to be 1.75, and  $H_{ii}$  and  $H_{jj}$  are the potential energies of states  $i$  and  $j$ , respectively. The interaction of the atomic sites is short-ranged, and therefore both the Hamiltonian and the overlap matrices are sparse. The dimensionality of these matrices in the systems in this study is  $\sim 20,000$ .

### Donor, acceptor, and bridge orbitals

In the calculation, all atoms in the whole protein are subdivided into donor, bridge, and acceptor complexes. The donor complex is composed of the side-chain structure of Trp<sup>306</sup> and a segment of the peptide backbone (NH-C<sub>α</sub>H-CO). The acceptor is a noncovalently attached FADH molecule. The other atoms in the protein are considered to be part of the bridge. The analysis of the donor-bridge-acceptor model is similar to that of our previous work (Daizadeh et al., 1997; Gehlen et al., 1996). The only difference between photolyase and the previously analyzed Ru-modified cytochrome  $c$  and azurin molecules, in which electron transfer occurs between metal ions, is that in the present case the donor and acceptor complexes are polyatomic.

In this case, an additional computational step is required. The donor and acceptor molecular orbitals are some linear combinations of the atomic orbitals of the respective complexes. These combinations are determined in a separate extended Hückel calculation. In this case the broken chain of the backbone of Trp<sup>306</sup> was modified by adding H and OH to form -NH<sub>2</sub> and -COOH termini. The donor molecular orbital is the HOMO of Trp<sup>306</sup>. The accepting orbital of \*FADH is the HOMO-1 of FADH, which becomes singly occupied upon the excitation of the molecule. (The singly occupied HOMO of FADH lies  $\sim 1$  eV higher than the ground state of the tryptophan and therefore is not likely to become an accepting orbital in this reaction.)

The coefficients of expansions of these molecular orbitals,  $\eta_i^d$  and  $\eta_j^a$ , are used to construct the zeroth-order donor and acceptor electronic states,

$$|d\rangle = \sum_i \eta_i^d |i\rangle \quad (5)$$

and

$$|a\rangle = \sum_j \eta_j^a |j\rangle, \quad (6)$$

which are embedded in the protein medium and weakly interact with each other via mutual coupling to the bridge.

### PROTEIN PRUNING

The electronic communication between donor and acceptor complexes (Trp<sup>306</sup> and FADH, respectively) is mediated by a small number of structural units (amino acids) of the protein. The goal of the procedure described in this section is to identify those important units. The method used is the following. We calculate the electronic coupling for the whole protein and then eliminate those amino acids that are not affecting the electronic coupling. The numerical strategy usually involves two steps (Gehlen et al., 1996): protein truncation and protein pruning. Below we describe a numerical procedure for the calculation of the electronic coupling matrix element and those for truncation and protein pruning.

### Full protein calculation

In the extended Hückel model the coupling coefficients of the donor and acceptor states to the bridge are given by

$$V_{ai} = \langle a | (H - E_0 S) | i \rangle, \quad V_{jd} = \langle j | (H - E_0 S) | d \rangle, \quad (7)$$

where  $E_0$  is the tunneling energy, which in our calculations was set at  $-12$  eV, the energy of both donor and acceptor states. These expressions can be evaluated by using the expansion coefficients of the  $|d\rangle$  and  $|a\rangle$  states (Eqs. 5 and 6) and the elements of the Hamiltonian and the overlap matrices in the atomic basis set. The electronic Green's function matrix elements are

$$G_{ij} = (E_0 S - H)_{ij}^{-1}. \quad (8)$$

In actual calculations the inversion of the matrix is avoided by rewriting the expression for electronic coupling in terms of the transition amplitudes  $R_i$ :

$$T_{DA} = \sum_i V_{ai} R_i, \quad (9)$$

where the unknown transition amplitudes are computed by solving the system of linear equations:

$$V_{jd} = \sum_i (E_0 S_{ji} - H_{ji}) R_i. \quad (10)$$

The implementation of the method is described in detail by Daizadeh et al. (1997). Because the Hamiltonian and the overlap matrices are sparse, and the numerical procedure of evaluating the matrix element involves only basic linear operations, extremely large systems can be treated with this method.

### Protein truncation: tunneling tube

Our goal in truncation is to rapidly remove those parts of the original protein molecule that are not important for the electron transfer process. Because most of the amino acids are spatially far away from the electron transfer pathway, they are expected to be irrelevant to the electron tunneling mechanism. The portion of the protein relevant to the tunneling mechanism is chosen as follows. A cylinder of cross-sectional radius  $R$  with an axis defined by a straight line connecting donor and acceptor is created. The cylinder is capped on both sides with hemispheres of the same radius  $R$ . All amino acids that have at least one atom inside of the cylinder are retained, and others are removed from the original molecule; thus a truncated protein is created.

The remaining structure is modified by adding hydrogens to N or C termini on the ruptured ends of the peptide chain, yielding  $-NH_2$  or  $-COH$  termini, respectively. An extended Hückel evaluation of the matrix element for this truncated protein is then performed with the method of transition amplitudes. The goal is to find the minimum radius  $R$  of this tube such that the matrix element of the full protein can be reproduced. All matrix elements shown in Fig. 1 were computed with the method of transition amplitudes, as given by Eqs. 7, 9–10 with a tunneling energy of  $-12$  eV, which roughly corresponds to the energy of donor and

acceptor states evaluated within the extended Hückel model. The matrix element converged at  $R \approx 10$  Å, which suggested that all of the important amino acids are localized within the truncated protein. The truncation procedure is an extremely useful first step in reducing the protein to a relatively small object, which is further subjected to pruning described in the next section.

### Amino acid tunneling spectra and protein pruning

In the pruning procedure, the importance of individual amino acids is examined, and unimportant amino acids are removed from the molecule. When an amino acid is removed, the ruptured ends of the polypeptide backbone of the remaining structure are modified by adding hydrogens to the  $-NH$  and  $-CO$  termini to make  $-NH_2$  or  $-COH$  groups, respectively. The importance of individual amino acids is evaluated with a parameter  $p_\alpha$ :

$$p_\alpha = \left| \frac{T_{DA}^{(\alpha)} - T_{DA}}{T_{DA}} \right|. \quad (11)$$

Here  $T_{DA}^{(\alpha)}$  is the tunneling matrix element of the system calculated with one amino acid  $\alpha$  removed from the protein. This value is compared with the reference tunneling matrix element of the full protein,  $T_{DA}$ . The procedure is repeated until all amino acids have been examined. It is clear that if an amino acid is important, then its  $p_\alpha$  will be on the order of unity. All unimportant amino acids will have small values of  $p_\alpha$ . In the pruning procedure, an amino acid is removed permanently from the molecule if the value of  $p_\alpha$  is smaller than some threshold value,  $p_{cut}$ , which in our calculations was set at 0.1. The matrix elements were calculated as described in the previous section.

The spectrum of values of  $p_\alpha$ , which we refer to as the amino acid tunneling spectrum, gives information about the most important amino acids and therefore elucidates the pathway of electron transfer at the "amino acid resolution." In Fig. 2 the amino acid tunneling spectrum of Trp<sup>306</sup>-to-FADH transition in photolyase is shown. There are two large peaks on Trp<sup>359</sup> and Trp<sup>382</sup> where  $p_i$  is over 0.5. This result indicates that the major electron transfer pathway intensively relies on these two particular amino acids.

These two amino acids are located on the axis between donor Trp<sup>306</sup> and acceptor FADH. The closest distance between donor and Trp<sup>359</sup>, Trp<sup>359</sup> and Trp<sup>382</sup>, and Trp<sup>382</sup> and the flavin molecule, is  $\sim 3$  Å. Their orientation, as given by the crystal structure, is very interesting. The two indole groups appear to be nearly symmetrical along the main axis between donor and acceptor. The normal vectors of Trp<sup>306</sup> and Trp<sup>359</sup> are nearly perpendicular. On the other side, the normal vectors of Trp<sup>382</sup> and flavin are also nearly orthogonal. There is no doubt that in a real system at room temperature, this geometry will be distorted by thermal fluctuations of the protein structure, resulting in some variation of the tunneling paths. However, it is unlikely that

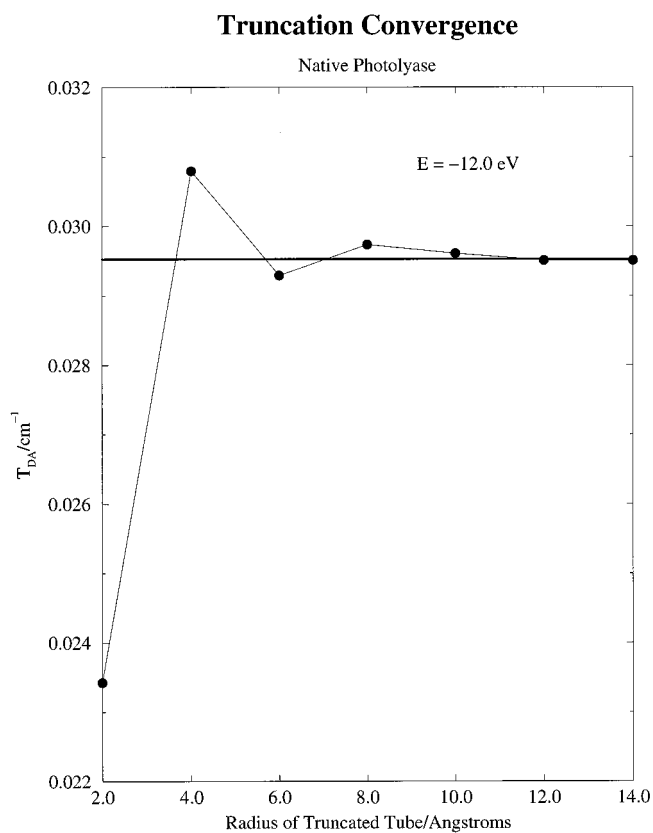


FIGURE 1 Convergence of the tunneling matrix element with the radius of the truncation tube. Protein truncation reveals that the matrix element is fully converged at about 10 Å.

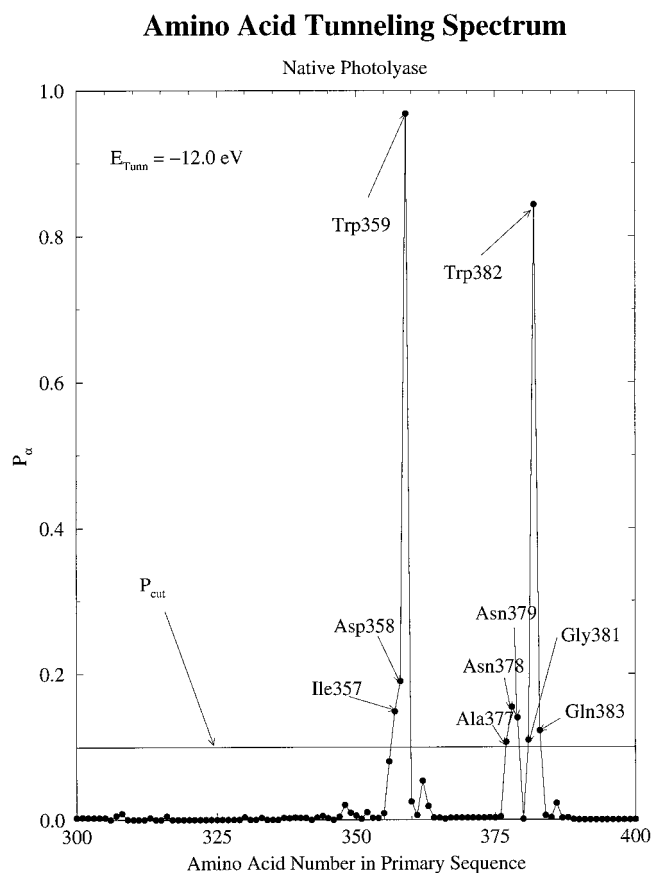


FIGURE 2 Amino acid tunneling spectrum of native photolyase. It is seen that only nine amino acids contribute substantially to the tunneling process with a  $p_{\alpha} \bar{n}$

thermal fluctuations will destroy the major features of the amino acid tunneling path obtained in the calculation. Further insights into the mechanism of electron transfer in this system can be obtained with the method of tunneling currents, which we discuss in the next section. With this method the tunneling pathways can be examined with “atomic resolution.”

## TUNNELING CURRENTS AND PATHWAYS

Once the most important amino acids constituting the tunneling pathway have been identified, further, more detailed analysis can be carried out with the method of interatomic tunneling currents. This method allows one to get insight into the atomic details of the tunneling process, that is, to determine which atoms of the protein are involved in promoting the tunneling electron and to what extent, and to determine the tunneling pathways at the atomic level of resolution. The method is described in detail by Stuchebrukhov (1996, 1997). Here we discuss the main expressions that are used in the calculation and present the results for photolyase.

## Diabatic donor and acceptor states

In contrast to the matrix element evaluation, the calculation of the tunneling currents involves a diagonalization procedure. Because the pruned protein is relatively small, diagonalization can be easily performed and the eigenstates of the system found. The key role in the analysis is played by two eigenstates that correspond to so-called diabatic donor and acceptor electronic states. These states are formed as a result of partial delocalization of the donor and acceptor orbitals (found as eigenstates of isolated donor and acceptor complexes) in the medium because of the interaction of the donor and acceptor complexes with the local protein environment. (Rigorously speaking, the electronic eigenstates determined at fixed nuclear coordinates are usually called adiabatic states. However, when there is no significant mixing of the donor and acceptor states, the localized adiabatic eigenstates practically coincide with the diabatic states (Newton, 1991)). The molecular orbitals  $|d\rangle$  and  $|a\rangle$  are the zeroth-order approximations for diabatic donor,  $|D\rangle$ , and acceptor,  $|A\rangle$ , states. These diabatic states can be identified by projecting all eigenstates  $|\lambda\rangle$  of the pruned protein onto the donor and acceptor orbitals,  $|d\rangle$  and  $|a\rangle$ , and selecting two eigenstates that have maximum overlap with the donor and acceptor molecular orbitals:

$$|\langle d|D\rangle| = \max_{\lambda} |\langle d|\lambda\rangle| \quad (12)$$

and

$$|\langle a|A\rangle| = \max_{\lambda} |\langle a|\lambda\rangle|. \quad (13)$$

The coefficients of expansion of the donor and acceptor states in terms of the atomic basis of the protein can then be determined:

$$|D\rangle = \sum_i C_i^D |i\rangle \quad (14)$$

and

$$|A\rangle = \sum_j C_j^A |j\rangle. \quad (15)$$

These coefficients,  $C_i^D$  and  $C_j^A$ , are used in the calculations of the atomic tunneling currents.

## Interatomic tunneling currents: atomic resolution of the tunneling pathway in photolyase

The tunneling current between two particular orbitals on neighboring atoms  $a$  and  $b$  during the tunneling transition is defined by (Stuchebrukhov, 1997)

$$J_{ai,bj} = \frac{1}{\hbar} (H_{ai,bj} - E_0 S_{ai,bj}) (C_{ai}^A C_{bj}^D - C_{ai}^D C_{bj}^A), \quad (16)$$

where in the notation of the atomic states we have introduced a second index referring to different atoms, so that, for example, the double index  $ai$  refers to the  $i$ th orbital on the  $a$ th atom. The two states  $|D\rangle$  and  $|A\rangle$  are assumed to have

the same tunneling energy  $E_0$ . In the calculation, an external electric field was applied to shift states  $|D\rangle$  and  $|A\rangle$  from their initial positions to bring them close to a resonance. This shift of the energies of donor and acceptor states is a simulation of the effect of the polar solvent and local molecular environment in an ET reaction (Marcus and Sutin, 1985).

The total tunneling current between two atoms  $a$  and  $b$  is a sum of currents between all orbitals of these two atoms:

$$J_{a,b} = \sum_{i \in a} \sum_{j \in b} J_{ai,bj} \quad (17)$$

Analysis of the matrix of interatomic currents  $J_{ab}$  yields detailed information about the structure of the tunneling flow and allows for a description of the tunneling pathways in a rigorous and quantitative fashion. The absolute value of the current  $J_{ab}$  is proportional to the probability that the tunneling electron on the way from donor to acceptor will pass from a given atom  $a$  to atom  $b$ . The positive sign of  $J_{ab}$  means that the current is directed from  $b$  to  $a$ ; the negative sign corresponds to the opposite direction of the current.

One particularly useful atomic characteristic of the tunneling flow is the total tunneling current through an atom:

$$J_a^+ = \sum_b J_{a,b} \quad (18)$$

The total current  $J_a^+$  through an atom  $a$  is a sum of all currents flowing into it. The prime on the sum means that only positive currents from the neighboring atoms  $b$  are selected, i.e., all terms in the sum are positive,  $J_{a,b} > 0$ . For atoms of the intervening protein medium, the total current,  $J_a = J_a^+ + J_a^-$ , is zero, meaning that the current flowing into atom  $a$ ,  $J_a^+$ , equals in absolute value and is opposite in sign to that of the current flowing out,  $J_a^-$ , according to conservation of electric charge. The numerical value of the total current  $J_a^+$  is proportional to the average number of times that the tunneling electron will pass a given atom on its way from donor to acceptor,  $N_a$ . The proportionality coefficient coincides with the value of the tunneling matrix element:

$$N_a = \frac{\hbar J_a^+}{|T_{DA}|} \quad (19)$$

This number, which we call the tunneling count, can be greater than unity because the tunneling flow can include circular currents (Stuchebrukhov, 1996, 1997).

In Fig. 3, the distribution of the tunneling counts  $N_a$  for electron transfer between Trp<sup>306</sup> and FADH for a 6-Å truncated tube of photolyase at the tunneling energy of -12 eV is shown. The tunneling currents are seen to be mostly localized on the donor Trp<sup>306</sup>, Trp<sup>359</sup>, Trp<sup>382</sup>, and acceptor FADH, which is in agreement with the amino acids selected from the pruning technique. It is also seen that the tunneling electron passes through some atoms several times on its way from donor to acceptor. In Fig. 4, atoms and their half-bonds are colored in red, with intensity proportional to the total atomic tunneling current flowing through each atom (or to

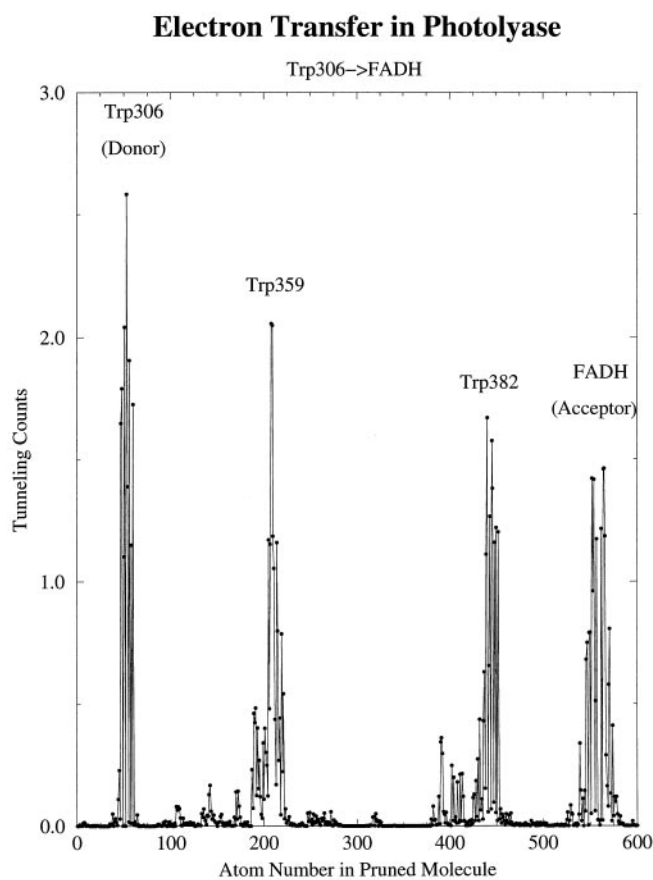


FIGURE 3 Tunneling counts in the Trp<sup>306</sup>-to-FADH electron transfer process. Tunneling counts refer to Eq. 19 and physically correspond to the average number of times that a tunneling electron will pass a given atom on its way from the donor to the acceptor complex. It is seen that the major contributors are atoms from the donor and acceptor complexes and the Trp<sup>359</sup> and Trp<sup>382</sup> amino acids. The tunneling counts can be greater than 1.0 if they involve circular currents (see text).

their corresponding tunneling counts) (Eq. 19). If we zoom in on the atomic detail of the electron transfer pathways, we obtain Fig. 5, which shows the details of how electrons flow through a set of aromatic structures starting from the indole group of the donor Trp<sup>306</sup>, then to Trp<sup>359</sup> and Trp<sup>382</sup>, and finally reaching the flavin group of the acceptor FADH. Thus we see that the electron transfer pathway between Trp<sup>306</sup> and FADH in photolyase involves the intermediate aromatic amino acids Trp<sup>359</sup> and Trp<sup>382</sup>. These amino acids provide the bridge between donor and acceptor by a set of orthogonally overlapped  $\pi$  rings.

In the past, the tunneling pathway for this electron transfer in photolyase has been probed experimentally in site-directed mutagenesis studies by replacing the tryptophans with phenylalanines (Li et al., 1991). To investigate the effect of mutations, we artificially modified the native photolyase molecule into W359F and W382F mutants by using the computer modeling program SCRWL (SCRWL stands for side-chain placement with a rotamer library) (Bower et al., 1997). The two mutants were pruned as discussed in the previous section, and then we performed the current

## Currents in *E. coli* Photolyase

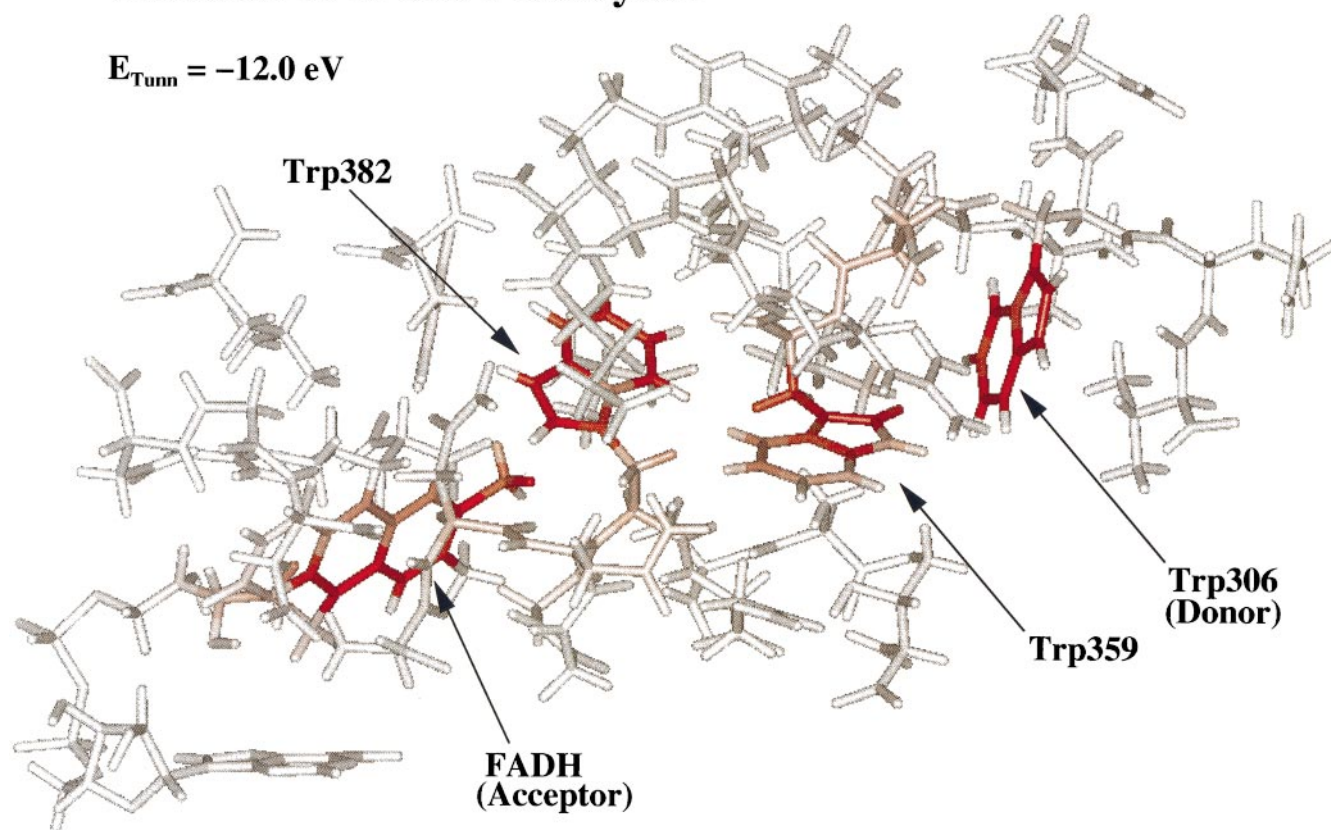


FIGURE 4 Total tunneling currents in native *E. coli* photolyase at a tunneling energy of  $-12.0 \text{ eV}$ . It is seen that the tunneling current is most strongly located on only four amino acids, which lie directly between donor and acceptor complexes.

analysis on these pruned systems. We find that Phe<sup>359</sup> strongly participates in the pathway and is a functional substitution for Trp<sup>359</sup> in the electron transfer process. Similarly, we find that Phe<sup>382</sup> is also a functional mutant in the sense that the tunneling currents are still localized on the modified amino acid, which plays the role of one of two intermediates, in a way similar to that of Trp<sup>382</sup> in the native molecule. These results indicate that electron transfer in these systems is strongly dependent on the aromaticity of the pathway.

Although we find that the pathway in the mutants looks almost identical to that of the native molecule in the sense that the substituted phenylalanines play the role of intermediates in electron transfer, we find, however, that  $|T_{\text{DA}}|$  is significantly smaller. The coupling matrix element for the native molecule was calculated to be on the order of  $5 \times 10^{-2} \text{ cm}^{-1}$ , which corresponds to a maximum electron transfer rate constant,  $k_{\text{max}}$ , on the order of  $10^6 \text{ s}^{-1}$ , for a typical reorganization energy of  $0.5 \text{ eV}$ . The electronic coupling matrix element for the site-directed mutants was calculated to be smaller by a factor between 5 and 10, depending on the configuration of the site substitutions. Despite the drop in the electronic coupling, these mutations do not completely disrupt the electronic communication between Trp<sup>306</sup> and FADH. And if the Trp<sup>306</sup>-to-FADH

electron transfer is not a rate-limiting step in the photoactivation process, these mutations would not be noticeable. In recent experimental studies, however, it was found that the electron transfer rate constant in these mutants goes up by a factor of 2 (Özer and Sancar, unpublished results). On the other hand, it is clear that because the phenylalanines are much smaller and their virtual orbitals are much higher in energy than those of tryptophans, these substitutions without relaxation of the structure of the protein matrix around these sites cannot increase the electronic coupling between Trp<sup>306</sup> and FADH. This is precisely what our calculations show. It is also unlikely that these substitutions will significantly change the reorganization energy or the driving force in this reaction. Therefore, the most likely explanation for the experimental findings of Özer and Sancar is the structural change of the protein matrix induced by the mutations, which may result in a decrease in the overall distance between donor and acceptor. To verify this hypothesis, however, further, more detailed studies are needed.

## DISCUSSION AND CONCLUSIONS

In the present study, we have demonstrated the applicability of the new computational methods of pruning and inter-

## Tunneling Currents in *E. coli* Photolyase

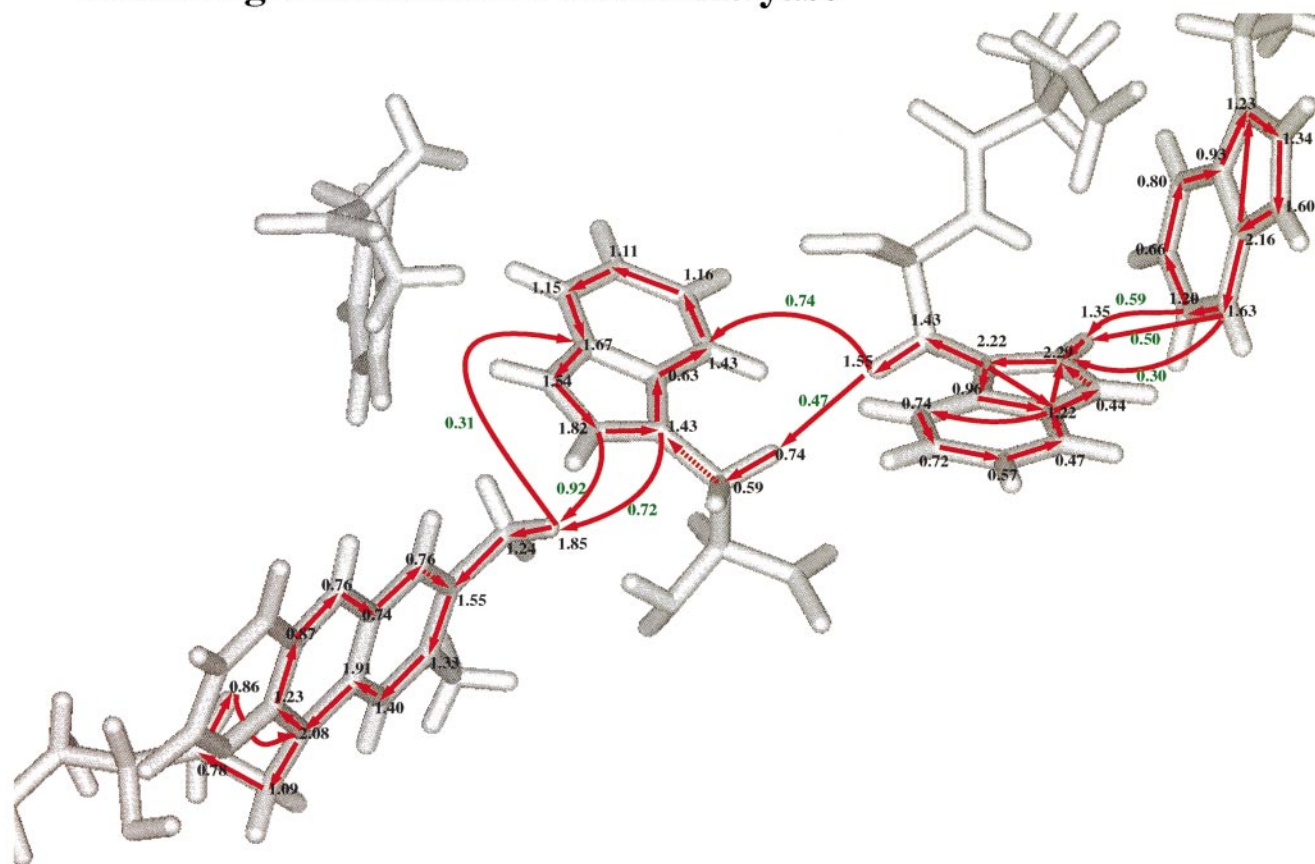


FIGURE 5 A closer view of the total tunneling current in the native protein. Analysis of  $J_{a,b}$  gives both magnitude and directionality of the tunneling flow. Circular currents are clearly seen in the Trp<sup>359</sup> and Trp<sup>382</sup> residues, as well as the donor and acceptor complexes.

atomic currents for the analysis of electron transfer pathways in a very large electron transfer system. The new methods allowed us to elucidate the long-range electron transfer pathway between Trp<sup>306</sup> and FADH in *E. coli* photolyase, a molecule that contains more than 7500 atoms. From our computational results, we find that these pathways involve the aromatic rings of two intervening tryptophans, Trp<sup>359</sup> and Trp<sup>382</sup>, whose  $\pi$  rings of the indole groups are oriented favorably to have strong overlaps with donor and acceptor, respectively. Compared to other electron transfer proteins, these pathways do not involve any continuous secondary structures. We find that the replacement of Trp<sup>359</sup> or Trp<sup>382</sup> with phenylalanines does not completely destroy the electron transfer pathway, but leads to a decrease in the electronic coupling.

The pathways analyzed in this paper are in a molecular "frozen" state; i.e., the thermal fluctuations were not included in the calculations. How strongly the details of such pathways will be affected by the thermal fluctuations of the molecule remains an open question (Daizadeh et al., 1997). It is unlikely, however, that the general features of the pathways found in the present static calculations, that is, the pathway at the amino acid level of resolution, will be completely destroyed by the thermal molecular motion. The

analysis of the mutants that were generated in this study revealed that an increasing number of important amino acids appear to accompany the replacement of tryptophans with phenylalanines. For example, Arg<sup>358</sup> in the W359F molecule and Asn<sup>378</sup> and Asn<sup>379</sup> in the W382F mutant photolyase become more important than in the native protein (see Fig. 1). Thus, the decrease in size of the aromatic ring results in greater delocalization of the electron during the tunneling process. It can also be interpreted as an increasing number of important pathways, according to an approach developed by Beratan and Onuchic (Onuchic et al., 1992).

Analysis of electron transfer pathways by full implementation of the method of this study is feasible for other large redox-related proteins that included either metal atoms or nonmetallic cofactors, as does photolyase. The method is a powerful theoretical tool that allows one to analyze quantitatively the electron transfer pathways in proteins at the atomic level of resolution. Efforts are currently under way in this group to elucidate the pathways of electron transfer from the excited flavin cofactor in photolyase to DNA, which contains a thymine dimer in a photolyase/DNA complex, the process central for biological function of the photolyase molecule.

We are grateful to Dr. Jens Antony for a series of stimulating discussions, and to Professor Aziz Sancar for permission to reference his unpublished results.

This work was supported by a research grant from the National Institutes of Health (GM54052-02) and by the fellowships from the Sloan and Beckman Foundations. Calculations presented in this paper were performed on the CRAY supercomputer provided by the Jet Propulsion Laboratory, Pasadena, California, and their contributions are gratefully acknowledged.

## REFERENCES

- Bower, M. J., F. E. Cohen, and R. L. Dunbrack. 1997. Prediction of protein sidechain rotamers from a backbone-dependent rotamer library: a new homology modeling tool. *J. Mol. Biol.* 267:1268–1282.
- Casimiro, D. R., J. H. Richards, J. R. Winkler, and H. B. Gray. 1993. Electron transfer in ruthenium-modified cytochromes-*c*-sigma-tunneling pathways through aromatic residues. *J. Phys. Chem.* 97:13073–13077.
- Daizadeh, I., J. N. Gehlen, and A. A. Stuchebrukhov. 1997. Calculation of electronic tunneling matrix element in proteins: comparison of exact and approximate one-electron methods for Ru-modified azurin. *J. Chem. Phys.* 106:5658–5666.
- Daizadeh, I., E. S. Medvedev, and A. A. Stuchebrukhov. 1997. Effect of protein dynamics on biological electron transfer. *Proc. Natl. Acad. Sci. USA.* 94:3703–3708.
- Gehlen, J. N., I. Daizadeh, A. A. Stuchebrukhov, and R. A. Marcus. 1996. Tunneling matrix element in Ru-modified blue copper proteins: pruning the protein in search of electron transfer pathways. *Inorg. Chem. Acta.* 243:271–282.
- Harm, W. 1980. *Biological Effects of Ultraviolet Radiation.* Cambridge University Press, New York.
- Heelis, P. F., R. F. Hartman, and S. D. Rose. 1995. Photoenzymatic repair of UV damaged DNA: a chemist's perspective. *Chem. Soc. Rev.* 24: 289–297.
- Husain, I., J. Griffith, and A. Sancar. 1988. Thymine dimers bend DNA. *Proc. Natl. Acad. Sci. USA.* 85:2558–2562.
- Johnson, J. L., S. Hamm-Alvarez, G. Payne, G. B. Sancar, K. V. Rajagopalan, and A. Sancar. 1988. Identification of the second chromophore of *Escherichia coli* and yeast DNA photolyases as 5,10-methenyltetrahydrofolate. *Proc. Natl. Acad. Sci. USA.* 85:2046–2050.
- Kanai, S., R. Kikuno, H. Toh, H. Ryo, and T. Todo. 1997. Molecular evolution of the photolyase-blue-light photoreceptor family. *J. Mol. Evol.* 45:535–548.
- Katz, D. J., and A. A. Stuchebrukhov. 1998. A new expression for superexchange matrix element in long-distance electron transfer reactions. *J. Chem. Phys.* 109:4960–4970.
- Kim, S.-T., Y.-F. Li, and A. Sancar. 1992. The third chromophore of DNA photolyase: Trp-277 of *Escherichia coli* DNA photolyase repairs thymine dimers by direct electron transfer. *Proc. Natl. Acad. Sci. USA.* 89:900–904.
- Kim, S.-T., and A. Sancar. 1991. Effect of base, pentose, and phosphodiester backbone structures on binding and repair of pyrimidine dimers by *Escherichia coli* DNA photolyase. *Biochemistry.* 30:8623–8630.
- Kim, S.-T., and A. Sancar. 1993. Photochemistry, photophysics, and mechanism of pyrimidine dimer repair by DNA photolyase. *Photochem. Photobiol.* 57:895–904.
- Kim, S.-T., A. Sancar, C. Essenmacher, and G. T. Babcock. 1993. Time-resolved EPR studies with DNA photolyase: excited-state FADH<sup>0</sup> abstracts an electron from Trp-306 to generate FADH<sup>-</sup>, the catalytically active form of the cofactor. *Proc. Natl. Acad. Sci. USA.* 90:8023–8027.
- Kuznetsov, A. M. 1995. *Charge Transfer in Physics, Chemistry, and Biology.* Gordon and Breach, Amsterdam.
- Langen, R., I. Chang, J. P. Germanas, J. H. Richards, J. R. Winkler, and H. B. Gray. 1995. Electron tunneling in proteins—coupling through a beta strand. *Science.* 268:1733–1735.
- Li, Y.-F., P. F. Heelis, and A. Sancar. 1991. Active site of DNA photolyase: tryptophan-306 is the intrinsic hydrogen atom donor essential for flavin radical photoreduction and DNA repair in vitro. *Biochemistry.* 30:6322–6329.
- Marcus, R. A., and N. Sutin. 1985. Electron transfers in chemistry and biology. *Biochem. Biophys. Acta.* 811:265–322.
- McConnell, H. M. 1961. Intramolecular charge transfer in aromatic free radicals. *J. Chem. Phys.* 35:508–515.
- Miaskiewicz, K., J. Miller, M. Cooney, and R. Osman. 1996. Computational simulations of DNA distortions by a *cis,syn*-cyclobutane thymine dimer lesion. *J. Am. Chem. Soc.* 118:9156–9163.
- Newton, M. D. 1991. Quantum chemical probes of electron-transfer kinetics—the nature of donor acceptor interactions. *Chem. Rev.* 91:767–792.
- Onuchic, J. N., D. N. Beratan, J. R. Winkler, and H. B. Gray. 1992. Electron-tunneling pathways in proteins. *Science.* 258:1740–1741.
- Özer, Z., J. T. Reardon, D. S. Hsu, K. Malhotra, and A. Sancar. 1995. The other function of DNA photolyase: stimulation of excision repair of chemical damage to DNA. *Biochemistry.* 34:15886–15889.
- Park, H. W., S.-T. Kim, A. Sancar, and J. Deisenhofer. 1995. Crystal structure of DNA photolyase from *Escherichia coli*. *Science.* 268: 1866–1872.
- Payne, G., P. F. Heelis, B. R. Rohrs, and A. Sancar. 1987. The active form of *Escherichia coli* DNA photolyase contains a fully reduced flavin and not a flavin radical, both in vivo and in vitro. *Biochemistry.* 26: 7121–7127.
- Sancar, A. 1994. Structure and function of DNA photolyase. *Biochemistry.* 33:2–9.
- Sancar, A. 1996. DNA excision repair. *Annu. Rev. Biochem.* 65:43–81.
- Sancar, G. B., F. W. Smith, and A. Sancar. 1985. Binding of *Escherichia coli* DNA photolyase to UV-irradiated DNA. *Biochemistry.* 24: 1849–1855.
- Stuchebrukhov, A. A. 1996a. Tunneling currents in electron transfer reactions in proteins. *J. Chem. Phys.* 104:8424–8432.
- Stuchebrukhov, A. A. 1996b. Tunneling currents in electron transfer reactions in proteins. II. Calculation of electronic superexchange matrix element and tunneling currents using nonorthogonal basis sets. *J. Chem. Phys.* 105:10819–10829.
- Stuchebrukhov, A. A. 1997a. On the non-orthogonal basis set calculations of the bridge-mediated electronic matrix elements. *Chem. Phys. Lett.* 265:643–648.
- Stuchebrukhov, A. A. 1997b. Tunneling currents in proteins: nonorthogonal atomic basis sets and Mulliken population analysis. *J. Chem. Phys.* 107:6495–6498.
- Todo, T., H. Ryo, K. Yamamoto, H. Toh, T. Inui, H. Ayaki, T. Nomura, and M. Ikenaga. 1996. Similarity among the *Drosophila* (6–4) photolyase, a human photolyase homolog, and the DNA photolyase-blue-light photoreceptor family. *Science.* 272:109–112.
- Wangbo, M. H., M. Evain, T. Hughbanks, M. Kertesz, S. Wijeyesekera, C. Wilker, C. Zheng, and R. Hoffman. 1976. Extended Hückel Molecular and Crystal Calculations Acquired from Quantum Chemistry Program Exchange (QCPE), Indiana University, program no. 517.